MNRAS **476,** 5332–5340 (2018)
Advance Access publication 2018 March 9
doi:10.1093/mnras/sty587

The surface reactivity of acrylonitrile with oxygen atoms on an analogue of interstellar dust grains

Helen J. Kimber,† Jutta Toscano‡ and Stephen D. Price★
Chemistry Department, University College London, 20 Gordon Street, London WC1H0AJ, UK

Accepted 2018 February 26. Received 2018 February 18; in original form 2017 August 22

ABSTRACT

Experiments designed to reveal the low-temperature reactivity on the surfaces of interstellar dust grains are used to probe the heterogeneous reaction between oxygen atoms and acrylonitrile (C_2H_3CN, $H_2C{=}CH\text{-}CN$). The reaction is studied at a series of fixed surface temperatures between 14 and 100 K. After dosing the reactants on to the surface, temperature-programmed desorption, coupled with time-of-flight mass spectrometry, reveals the formation of a product with the molecular formula C_3H_3NO. This product results from the addition of a single oxygen atom to the acrylonitrile reactant. The oxygen atom attack appears to occur exclusively at the C=C double bond, rather than involving the cyano(-CN) group. The absence of reactivity at the cyano site hints that full saturation of organic molecules on dust grains may not always occur in the interstellar medium. Modelling the experimental data provides a reaction probability of 0.007 ± 0.003 for a Langmuir–Hinshelwood style (diffusive) reaction mechanism. Desorption energies for acrylonitrile, oxygen atoms, and molecular oxygen, from the multilayer mixed ice their deposition forms, are also extracted from the kinetic model and are 22.7 ± 1.0 kJ mol^{-1} (2730 ± 120 K), 14.2 ± 1.0 kJ mol^{-1} (1710 ± 120 K), and 8.5 ± 0.8 kJ mol^{-1} (1020 ± 100 K), respectively. The kinetic parameters we extract from our experiments indicate that the reaction between atomic oxygen and acrylonitrile could occur on interstellar dust grains on an astrophysical time-scale.

Key words: astrochemistry – stars: formation – ISM: abundances – ISM: molecules.

1 INTRODUCTION

The known universe is composed overwhelmingly of hydrogen and helium. Yet, despite this composition, around 200 different molecular species have been detected to date in the interstellar medium (ISM). A large proportion of these interstellar molecules are found within dense interstellar clouds (Bergin & Tafalla 2007). In these regions, the penetration depth of destructive ultraviolet (UV) light from surrounding stars is significantly smaller than the clouds' radii. That is, the destructive photons are completely absorbed by the molecules and dust making up the outer layers of these clouds, and the starlight cannot reach molecules located towards the clouds' centres. This absence of UV light, and the associated low rates of molecular photodissociation, means the gas temperature in dense interstellar clouds is comparable to the dust temperature (approximately 10–20 K) and molecular lifetimes are considerably extended in comparison with many other regions of the ISM. These extended molecular lifetimes, coupled with the low temperatures, allow icy mantles to form on the surface of the silicaceous and carbonaceous dust grains in the cloud; such grains typically make up about 1 per cent of a cloud's mass (Williams & Cecchi-Pestellini 2016). These icy mantles form not only by the accretion of gas-phase molecules on to the cold grain surfaces, but also by reactions which synthesize molecules *in situ*, on the surface of the dust grains. These icy mantles are primarily composed of water but can also include CO, CO_2, and a variety of simple organic molecules (e.g. methanol).

Acrylonitrile (CH_2CHCN), also known as vinylnitrile, propenenitrile or cyanoethylene, was the first molecule with a C=C double bond to be observed in the ISM (Gardner & Winnewisser 1975; Gerry, Yamada & Winnewisser 1979). In the ISM, acrylonitrile may be important in the process of forming prebiotic molecules, since hydrogenation of the cyanide group results in a C-N single bond. The C-N bond is often considered the most important bond in nature, due to its presence in amino acids. However, the hydrogenation of cyanide groups has been shown to be slow on surfaces under interstellar conditions (Theule et al. 2011). Acrylonitrile has

★ E-mail:s.d.price@ucl.ac.uk
† Present address: Institute of Chemical Sciences, William Perkin Building, Heriot-Watt University, Edinburgh EH144AS, UK.
‡ Present address: Physical and Theoretical Chemistry Laboratory, Department of Chemistry, University of Oxford, South Parks Road, Oxford 0X13QZ, UK.

been observed in several interstellar and circumstellar environments displaying, for example, column densities of 3×10^{12} cm^{-2} in the dense dark cloud TMC-1 (Matthews & Sears 1983; Johansson et al. 1984). Acrylonitrile is yet to be observed as a constituent of ices present in the ISM. However, pure acrylonitrile's desorption energy has recently been determined to be 35 kJ mol^{-1} (4200 K) (Toumi et al. 2016). A desorption energy above 10 kJ mol^{-1} (1200 K) results in effectively no thermal desorption from a surface at a temperature of 10–20 K, a temperature typical of interstellar dust in a dense interstellar cloud. Thus, since acrylonitrile is observed in the gas phase in the ISM, and has a desorption energy larger than 10 kJ mol^{-1}, it is likely that acrylonitrile will be present in interstellar ices.

In addition to its detection in the ISM, acrylonitrile has also been observed in Titan's atmosphere (Vuitton, Yelle & McEwan 2007; Willacy, Allen & Yung 2016) and such nitrile molecules are also detected in cometary comas (Hudson & Moore 2004). Since the temperature of Titan's surface is 94 K (Hudson & Moore 2004), the reactions we report in this paper are also relevant to this planetary environment. Studying the reactivity of acrylonitrile also provides a direct comparison between the reactivity of C=C and C≡N bonds on surfaces, under interstellar conditions. Both of these functional groups are contained in many of the molecules detected in the ISM. The cyanide group can be found in simple radicals such as CN, small molecules such as HCN, as well as long-chain cyanopolyynes (Bell et al. 1997, 1998;Theule et al. 2011). The above analysis provides a strong motivation for establishing the reaction pathways available to acrylonitrile on cold surfaces.

Recently, there has been considerable interest in the heterogeneous reactivity of oxygen atoms in the ISM. For example, O atoms have been shown to have a high diffusion coefficient on surfaces of astrochemical interest (Minissale et al. 2013a) and O atoms have been shown to react with ammonia to yield hydroxylamine (He et al. 2015b). Since O atoms are the third most abundant species in the ISM (Cartledge et al. 2004), it follows that this large diffusion coefficient may result in significant O atom reactivity on interstellar surfaces. Furthermore, it has been suggested that, at cloud densities larger than 10^4 cm^{-3}, O atom impacts on the surfaces of dust grains may be more frequent than H atom impacts; hence, under such conditions, the heterogeneous chemistry on the grain may be dominated by O atom reactivity (Congiu et al. 2014).

The experimentally determined desorption energies of O atoms from surfaces of astrochemical interest are significantly larger than predicted by theory. The interaction energy of an oxygen atom and pyrene (representative of a bridge site in graphite) has been calculated to be 11.6 kJ mol^{-1} (1400 K) (Bergeron et al. 2008), and astronomical models have previously estimated an O atom binding energy of 800 K (6.65 kJ mol^{-1}) (Hasegawa, Herbst & Leung 1992; Stantcheva, Shematovich & Herbst 2002; Garrod, Weaver & Herbst 2008). However, analysis of independent experiments has recently yielded O atom desorption energies of 14.0 ± 0.2 kJ mol^{-1}(1680 ± 24 K) (Kimber, Ennis & Price 2014), 1475 ± 225 K (12.3 ± 1.9 kJ mol^{-1}) (He & Vidali 2014) and 1760 ± 230 K (14.6 ± 1.9 kJ mol^{-1}) (Minissale, Congiu & Dulieu 2016). In addition, He & Vidali (2014) have directly observed O atoms during temperature-programmed desorption (TPD) experiments, determining O atom desorption energies of 1660 ± 60 K (13.8 ± 0.5 kJ mol^{-1}) and 1850 ± 90 K (15.4 ± 0.7 kJ mol^{-1}) for desorption from a porous amorphous water ice and from a bare amorphous silicate film, respectively. These inconsistencies between experiment and theory require the further investigation of the reactions and mobility of O atoms on surfaces of relevance to the ISM. Indeed, there has been considerable recent interest in the depletion of oxygen from the gas phase of the ISM (Jenkins 2009; Whittet 2010; Hincelin et al. 2011). This depletion of oxygen cannot be accounted for by oxygen atom incorporation into the grains themselves (Whittet 2010). It is possible that the reactions of oxygen atoms on the surface of interstellar dust grains and on their icy mantles, such as the reaction described in this paper, could provide a sink for oxygen in the ISM.

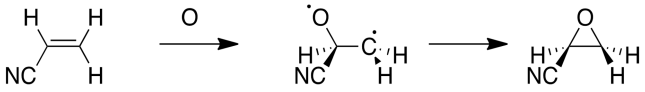

Figure 1. The reaction pathway of acrylonitrile and oxygen atoms in the gas phase.

In the gas phase, the major product channel from the reaction between acrylonitrile and oxygen atoms in their ground state (O ^{3}P) is thought to involve the formation of a biradical species (Fig. 1). As shown in Fig. 1, this biradical subsequently rearranges to form cyanoethyleneoxide, a molecule containing an epoxidering (Upadhyaya et al.1997). Minor reaction products from the gas-phase reaction involve the extraction of an H atom or a CN moiety from the acrylonitrile molecule by the incident O atom. Conventional transition state theory has been used to estimate an activation energy of 7.14 kJ mol^{-1} (859 K) for the gas-phase reaction between acrylonitrile and O atoms (Upadhyaya et al. 1997); this value indicates a significant barrier to reactivity at the low temperatures which are found in interstellar clouds. However, previous work shows that a heterogeneous environment, such as the surface of an interstellar dust grain, can provide alternative lower energy pathways for such atomic addition reactions (Ward & Price 2011). Thus, the significant barrier for the addition of O atoms to acrylonitrile in the gas phase is not necessarily an impediment to the reaction occurring on an interstellar surface.

2 EXPERIMENTAL

The experimental apparatus used in this study probes the reactions of atoms on the surfaces of molecular ices and has been described in detail before (Ward & Price 2011; Kimber, Ennis & Price 2014). Oxygen atoms are generated in the source chamber *via* a microwave discharge in O_2. The gas from the discharge is transported across the source chamber *via* a differentially pumped polytetrafluoroethylene (PTFE) dosing line. A second PTFE line is used to codose acrylonitrile (C_2H_3CN). The acrylonitrile was a commercial sample (Sigma–Aldrich, purity ≥ 99 per cent), degassed *via* multiple freeze-thaw cycles. The dosing lines enter a ultra-high vacuum (UHV) chamber where the flows of reactants are directed towards a sample of highly oriented pyrolytic graphite (HOPG). The dissociation efficiency of O_2 in the microwave discharge has been previously determined to be 20 per cent and, hence, the resulting gas is a mixture of O/O_2 (Ward & Price 2011). Previously, laser ionization has been employed to determine that the overwhelming majority of the reactant O atoms in the O/O_2 beam are in their ^{3}P ground state (Ward & Price 2011; Ward, Hogg & Price 2012) and studies of similar sources have shown that the vast majority of oxygen molecules in the O/O_2 beam are in their electronic ground state (Minissale, Congiu & Dulieu 2014). Previous experiments have also shown there is no detectable O_3 in the O/O_2 beam. This characterization of the O/O_2 beam is in agreement with other groups using similar microwave discharge cells to generate O atom beams (Minissale, Congiu & Dulieu 2014). In our experiments, the fluxes

of $O(^3P)$, O_2, and acrylonitrile to the HOPG surface are 0.27, 0.53, and 0.66 MLs^{-1}, respectively; where 1 ML = 1×10^{15}molecules cm^{-2} a standard measure of surface coverage. These flux determinations are supported by measurements of the time for a monolayer coverage to develop, using an identical source, in a new piece of apparatus incorporating a quadrupole mass spectrometer which has markedly improved sensitivity and is able to probe sub-monolayer coverages (Kimber 2016).

The HOPG surface is mounted on a closed-cycle helium cryostat which, when coupled with a tantalum strip heater, is capable of maintaining surface temperatures between 14 and 500 K; the temperature of 14 K is the lowest the surface can reach with the current cooling arrangement. During deposition, the substrate is held at a specific dosing temperature between 14 and 100 K. After 1 h of co-deposition, the dosing lines are evacuated and the surface is cooled from the dosing temperature to 14 K to ensure all TPD spectra are recorded under identical conditions. It is important to note that the dosing regime is such that the graphite surface is saturated within approximately 1 s. Therefore, the surface reaction occurs overwhelmingly on an acrylonitrile/oxygen matrix which reaches a thickness of the order of a thousand monolayers at the lowest surface temperatures. Final coverages of the dosed molecules, extracted from the kinetic model described below, are given in the Supporting Information. The products of the reaction are then detected using a TPD methodology involving time-of-flight mass spectrometry (TOFMS). During the TPD, the surface is heated by passing a current of 15 A through the heater. This heating sequentially desorbs the components of the molecular ice from the graphite substrate. A pulsed 200 eV electron beam passes through the source region of the TOFMS, located close to the surface, and ionizes a proportion of the desorbing molecules which are then detected by the TOFMS. To improve the mass spectral resolution, the energy of the electron beam is lower than that used in our previous work (Ward & Price 2011). Our experimental data set for a given dosing temperature comprises a two-dimensional array $I(m/z, T_{TPD})$; where any point in this array gives the ion counts I at a specific mass-to-charge (m/z) ratio and surface temperature (T_{TPD}) during the desorption heating ramp. Appropriate 'blank' spectra were also recorded at each dosing temperature. In these blank spectra only acrylonitrile and O_2 are dosed on to the surface and no incident O atoms are present. These blank spectra (Fig. 2) and other experiments performed during the commissioning of the atom source (Ward & Price 2011; Ward, Hogg & Price 2012), such as confirming that no products are formed if the O atom beam is directed away from the surface, confirm that the product signals in the experiment are due to the reactions of the O atoms with the molecules present on the graphite surface (Kimber, Ennis & Price 2014; Kimber 2016).

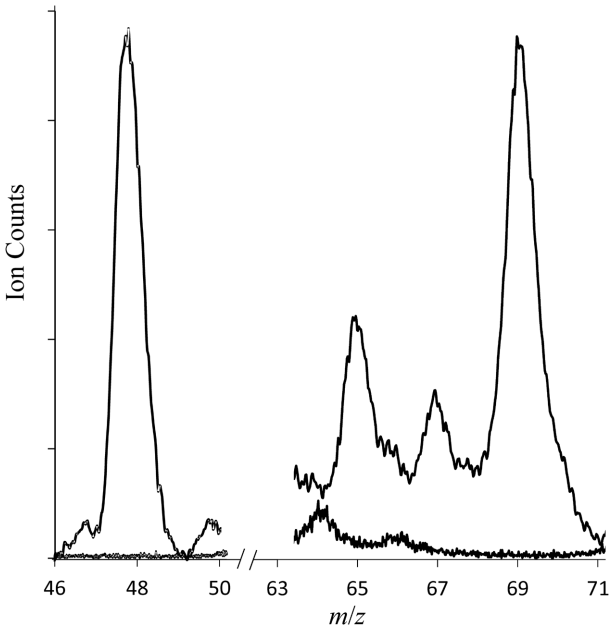

Figure 2. Sections of representative mass spectra recorded during the TPD phase of the experiments showing peaks for $m/z = 69$, corresponding to the additions of one oxygen atom to acrylonitrile, and $m/z = 48$ corresponding to O_3 formed in the competing reaction between O atoms and O_2. The lower traces in each section show the signals when dosing in an identical ('blank') experiment with no microwaves applied to the atom source; that is simply dosing with O_2 and acrylonitrile. The surface temperature during the dosing phase was 40 K. The vertical axis is linear. The mass spectra were collected over desorption temperature ranges of 67–72 K for mass 48 and 172–185 K for mass 69. See the text for details.

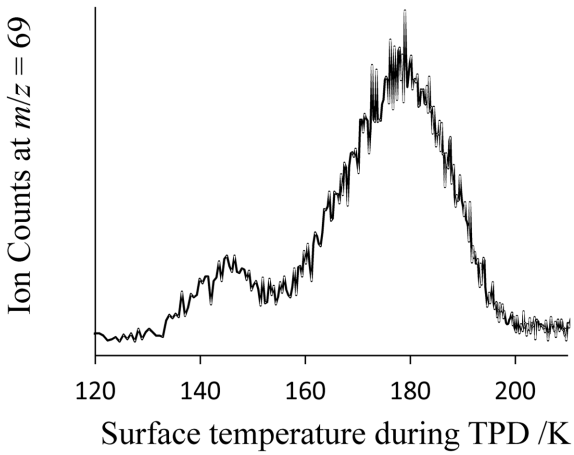

Figure 3. Representative desorption spectrum for $m/z = 69$ during the TPD heating phase.

3 RESULTS

Whenever acrylonitrile and O atoms are co-dosed on to the graphite surface, at surface temperatures below 100 K, a signal at $m/z = 69$ is observed in the mass spectra recorded during the TPD phase (Fig. 2). The signal at $m/z = 69$ is consistent with a species with the empirical formula C_3H_3NO, which indicates the addition of a single oxygen atom to an acrylonitrile molecule. The desorption profile (Fig. 3) of this single-addition product ($m/z = 69$) appears to contain two desorption features, a weaker desorption at a temperature of approximately 145 K and a stronger desorption centred at 178 K. These two desorption features hint that two isomers of the single-addition product might be formed on the surface, as discussed in more detail in the final paragraph of Section 5.

No other statistically significant signals corresponding to the reaction of O atoms with acrylonitrile are observed. Other alternative reaction products (e.g. HOCN) would readily be identified by desorption signals at different temperatures to that observed for $m/z = 69$ and the mass spectra associated with those desorption signals would have allowed their identification.

The yield of the single-addition product, for an experiment at a single dosing temperature T_D, is evaluated by first determining the

range of temperatures over which the product is desorbed during the TPD. Such a desorption spectrum (Fig. 3) shows that molecules with $m/z = 69$ desorb between 135 and 200 K. From our data array, we then generate a mass spectrum for the ions detected in the TPD data at surface temperatures (T_{TPD}) between 135 and 200 K (see Supporting Information). We then integrate the counts in the peak at $m/z = 69$ in this mass spectrum to give the raw ion yield for this individual experiment $R(69,T_D)$. To remove any potential contributions to the signals at $m/z = 69$ that are not due to the reaction of O atoms, we process a 'blank' TPD data set (no O reactant atoms present) in an identical manner to that used to derive $R(69,T_D)$. The very small number of ion counts at $m/z = 69$ (Fig. 2) in this blank spectrum, which are principally due to stray ions and electrical noise, are then subtracted from $R(69,T_D)$ to give the ion yield from the reaction at surface temperature T_D:$Y(69,T_D)$. This subtraction reduces $R(69,T_D)$ by typically less than 0.5 per cent when the product is desorbing, strongly supporting our conclusion that the product signals are due to the reaction of O atoms with acrylonitrile. The above procedure is repeated for a series of similar experiments performed at a range of dosing temperatures (T_D) between 14 and 100 K. In total three separate determinations of $Y(69,T_D)$ were made at each dosing temperature and averaged. The above procedure determines the relative yields of the product molecule at each dosing temperature.

When dosing at low surface temperatures (14–50 K) a peak at $(m/z) = 48$ is also observed in the mass spectra (Fig. 2). This signal arises from O_3 formed in the side-reaction of O atoms with undissociated O_2 on the surface (Minissale et al. 2013a; Congiu et al. 2014; Minissale, Congiu & Dulieu 2014). The peak at $(m/z) = 48$ is also integrated in the same fashion as described above to yield $Y(48,T_D)$.

As described in detail below, we have developed a kinetic model to reproduce the yields of the product molecules in our experiments. To compare the relative yields of C_3H_3NO and O_3 at each dosing temperature with our kinetic model we must convert the number of counts in our mass spectra to the number of molecules desorbing. This transformation is carried out by integrating the mass spectral signals, recorded in a TPD experiment, at $m/z = 53$ (C_2H_3CN) and $m/z = 32$ (O_2) from a known dose of acrylonitrile and O_2, deposited when the surface is held at a temperature of 14 K. The integrated signals at $m/z = 53$ and 32 then allow us to determine proportionality constants between the number of counts at these respective masses and the molecular abundance of acrylonitrile and O_2, respectively. These proportionality constants represent the detection efficiency of the parent molecule when acrylonitrile or O_2 desorbs from the surface and is ionized and detected by the TOFMS. This determination of the detection efficiency assumes a sticking probability of unity in the calibration experiment, which is the case at a surface temperature of 14 K. Indeed, the values of the detection efficiencies determined in this procedure have been supported by recent experiments using a modified experiment where dramatically improved sensitivity allows us to determine the monolayer coverage by the form of the desorption profile (Minissale, Congiu & Dulieu 2014; Kimber 2016). To determine the detection efficiency of O_3, from the value we determine for O_2, is straightforward, as the partial electron ionization cross-sections, and fragmentation patterns, at 200 eV of the two molecules are known (Newson et al. 1995; Straub et al. 1996). However, the electron ionization cross-section of the single-addition product must be assumed to be equal to that of a crylonitrile, since the relevant partial ionization cross-sections for any of the possible isomers of C_3H_3NO are unknown. When determining the detection efficiency of C_3H_3NO we must also allow

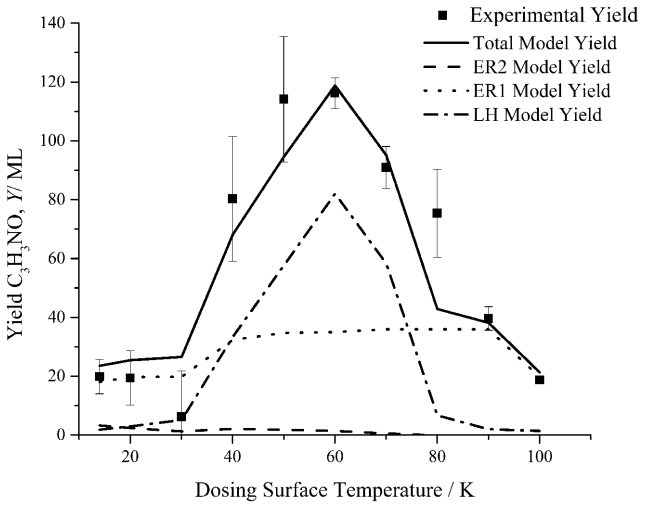

Figure 4. Yield of C_3H_3NO, formed following the codeposition of acrylonitrile (C_2H_3CN) and O atoms, as a function of surface temperature. Squares: experimental data; solid line: model; dashes: ER2 mechanism; dots: ER1 mechanism; and dot-dash: LH mechanism. The error bars associated with the experimental results represent two standard deviations from three repeats at each surface temperature.

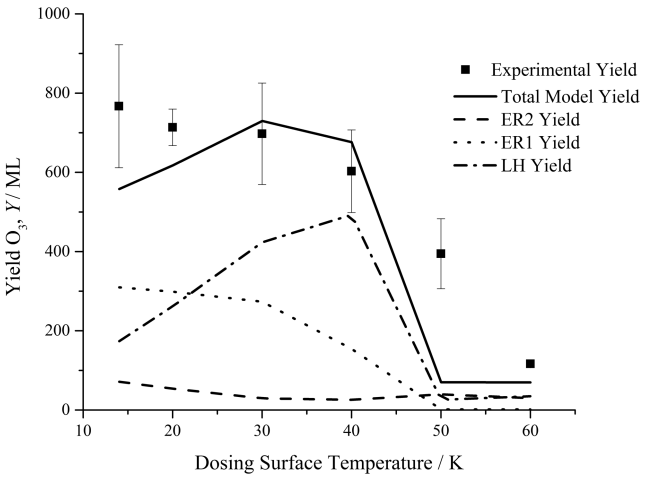

Figure 5. Yield of O_3 formed following the codeposition of acrylonitrile (C_2H_3CN) and O atoms, as a function of surface temperature. The error bars associated with the experimental results represent two standard deviations from three repeats at each surface temperature. Legend as in Fig. 4.

for the fact that not every molecule of the product or acrylonitrile ionized results in a parent ion in the mass spectrum; that is, we must allow for fragmentation in the ionization process. To make this correction for the product observed at $m/z = 69$, the fragment to parent ratio is estimated from the standard mass spectrum of acetylcyanide from the NIST reference database (Stein 2015) and the relative yield of parent ion ($m/z = 53$) to fragments for acrylonitrile is determined from our mass spectra. The above procedure allows the yield of C_3H_3NO and O_3 molecules from the relevant surface reactions to be estimated from our TPD data. The yield of products is reported, in ML given the known surface area, as a function of the surface temperature during the dosing.

The experimentally determined yields of C_3H_3NO and O_3 at each dosing temperature can be seen in Figs 4 and 5, respectively. The forms of Figs 4 and 5 will be discussed in the next section.

4 MODEL

A simple model can be used to extract kinetic parameters from our experimental data. The model is based on a methodology developed by Minissale et al. (2013b; Minissale, Congiu & Dulieu 2014) to account for the yield of ozone formed in the reaction between O atom beams (including O_2 molecules) and both O_2 and CO on surfaces of astrochemical interest. The current kinetic model extends considerably the earlier models we have used to characterize the multilayer ices generated in our experiments (Ward & Price 2011; Ward, Hogg & Price 2012; Kimber, Ennis & Price 2014).

The model involves the three branches of O atom reactivity which account for the yield of O_3 and C_3H_3NO we observe. First, the O atoms can react with one another to form molecular oxygen and, secondly, the O atoms can also react with molecular oxygen to form O_3 (Reactions 1 and 2).

$$\mathrm{O\,(ads) + O\,(ads) \rightarrow O_2\,(ads)} \quad (1)$$

$$\mathrm{O_2\,(ads) + O\,(ads) \rightarrow O_3\,(ads)} \quad (2)$$

Thirdly, the O atoms can react with acrylonitrile to form the single-addition product ($m/z = 69$) with the empirical formula C_3H_3NO (Reaction 3).

$$\mathrm{C_2H_3CN\,(ads) + O\,(ads) \rightarrow C_3H_3NO\,(ads)} \quad (3)$$

Minissale et al. (2013b; Minissale, Congiu & Dulieu 2014) have shown that in order to successfully model the yield of O_3 formed on surfaces of astrochemical interest, Reactions (1) and (2) must be effectively barrierless and the O atoms must have a significant diffusion coefficient. These earlier experiments also show that O_3 does not react with O atoms; that is, Reaction (4) is not a competing channel on the surface.

$$\mathrm{O_3\,(ads) + O\,(ads) \rightarrow 2O_2\,(ads)} \quad (4)$$

In principle, Reactions (1)–(3) can proceed *via* two possible reaction mechanisms on the surface: *via* a Langmuir–Hinshelwood (LH) pathway or *via* an Eley–Rideal (ER) pathway. The LH mechanism proceeds when both reactants are adsorbed and thermalized on the substrate, as written in the chemical equations above. The O atoms can then diffuse across the surface and react with another mobile O atom or with a heavier species, such as O_2 or acrylonitrile [as shown in Reactions (1)-(3)]; the heavier species are assumed to be immobile at the surface temperatures studied. The ER mechanism occurs when an adsorbed species undergoes a direct reaction with a species incident from the gas phase; the incident species is not adsorbed on the surface before the reaction. The reactants are co-dosed in the current experiments, so either reactant can be the adsorbed species or the gas-phase partner for an ER process. Hence, two ER pathways must be modelled. ER1 indicates the reaction where O atoms are the gas-phase reactant and the reaction partner is adsorbed on the surface, Reactions (5)–(7); ER2 denotes the reaction where O atoms are the thermalized surface reactant, Reactions (8) and (9).

$$\mathrm{O\,(ads) + O\,(g) \rightarrow O_2\,(ads)} \quad (5)$$

$$\mathrm{O_2\,(ads) + O\,(g) \rightarrow O_3\,(ads)} \quad (6)$$

$$\mathrm{C_2H_3CN\,(ads) + O\,(g) \rightarrow C_3H_3NO\,(ads)} \quad (7)$$

$$\mathrm{O\,(ads) + O_2\,(g) \rightarrow O_3\,(ads)} \quad (8)$$

$$\mathrm{O\,(ads) + C_2H_3CN\,(g) \rightarrow C_3H_3NO\,(ads)} \quad (9)$$

The rates for the LH and ER mechanisms are:

$$r_{\mathrm{LH,X}} = k_{\mathrm{diff}}\,\rho_{\mathrm{LH,X}}\,[\mathrm{X\,(ads)}]\,[\mathrm{O\,(ads)}] \quad (10)$$

$$r_{\mathrm{ER1,X}} = \rho_{\mathrm{ER1,X}}\,[\mathrm{X\,(ads)}]\,F_O \quad (11)$$

$$r_{\mathrm{ER2,X}} = \rho_{\mathrm{ER2,X}}\,[\mathrm{O\,(ads)}]\,F_X \quad (12)$$

In Reactions (10)–(12), r is the rate of the relevant reaction, where X = O, O_2, or C_2H_3CN, F_X represents the deposition flux of the relevant reactant and k_{diff} is the surface diffusion coefficient of the O atoms. By giving [X(ads)] and [O(ads)] as unitless fractional coverages, relative to the monolayer coverage, the LH and ER rate coefficients become unitless reaction probabilities, ρ (Minissale et al. 2013a,b; Congiu et al. 2014).

As described in the Supporting Information (S1), we integrate the rate equations governing the surface concentrations of the species involved in the above chemical equations. These rate equations involve deposition fluxes, the changes in species concentrations due to surface reactions and desorption.

The total yield of C_3H_3NO from this integration can then be compared with the experimental yield, at a given surface temperature. The reaction probabilities and desorption energies are varied to fit the model to the experimental data over the whole range of dosing temperatures. The reaction probabilities for the two complimentary ER pathways for a given reaction (ER1 and ER2) are assumed to be equal. This assumption seems logical and also reduces the number of free parameters in the model. The best fit obtained from the model is shown in Fig. 4. The fit was obtained using the parameter values listed in Table 1. As discussed above, the self-reaction of O atoms, and their reaction with O_2 have previously been shown to be barrierless (Minissale et al. 2013a; Congiu et al. 2014; Minissale, Congiu & Dulieu 2014); hence, reaction probabilities of unity are used for these processes.

Whilst it is possible to fit the temperature dependence of our experimental yield of C_3H_3NO using a value of k_{diff} which has an Arrhenius temperature dependence, such a temperature dependence for k_{diff} markedly underpredicts the yield of O_3 we observe at surface temperatures below 30 K. If O atoms are diffusing on the surface to form O_3, they must also encounter acrylonitrile molecules on the surface and so encounters between O atoms and acrylonitrile *via* the LH mechanism [Reaction (3)] must occur below 30 K. Hence, as with previous work, we model the temperature dependence of the rate of O atom diffusion by an empirical non-Arrhenius expression which reproduces the reactivity of O atoms on low-temperature surfaces (Minissale et al. 2013b; Congiu et al. 2014):

$$k_{\mathrm{diff}} = k_0\left(1 + {T_D}^3/{T_0}^3\right) \quad (13)$$

In equation (13), k_0 is 0.9 and T_0 is 10 K. Whilst the reaction we observe occurs largely on the surface of an acrylonitrile/O_2 ice, previous work has shown that the O atom diffusion coefficient is largely independent of the substrate (Congiu et al. 2014). The above expression for k_{diff} is employed in the modelling shown in Figs 4 and 5.

5 DISCUSSION

The fit obtained with our kinetic model (Fig. 4) shows that the dominant mechanisms for the formation of C_3H_3NO are the LH and ER1. The ER1 mechanism occurs between a gas-phase O atom and a thermalized surface acrylonitrile molecule. The ER2 mechanism is significantly less active than the ER1, since [O(ads)]≪[C_2H_3CN(ads)]

Table 1. Kinetic parameters characterizing the reaction of O atoms with acrylonitrile to form C_3H_3NO.

$E_{Des,O2}$/kJ mol^{-1} [/K]	$E_{Des,O}$/kJ mol^{-1} [/K]	$E_{Des,C2H3CN}$/kJ mol^{-1} [/K]	1000 ρ_{ER}	1000 ρ_{LH}
8.5 ± 0.8 [1020 ± 100]	14.2 ± 1.0 [1710 ± 120]	22.7 ± 1.0 [2730 ± 120]	38 ± 4	7 ± 3

Notes: As discussed in the text, these parameters have been extracted by adjusting the parameters of our model to fit the experimental data set.

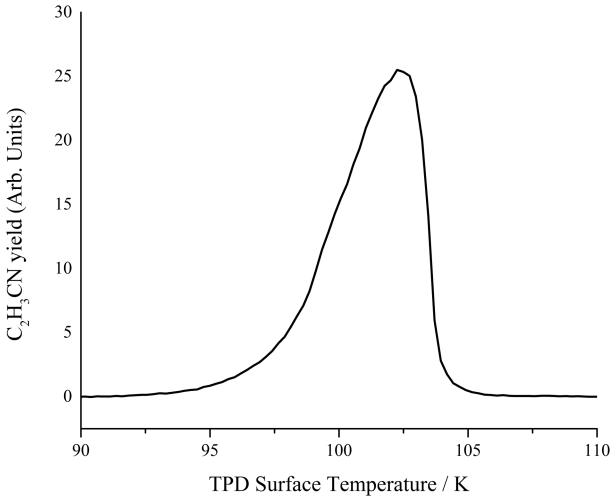

Figure 6. Desorption profile for C_2H_3CN desorbing from the surface during the TPD experiment.

despite their fluxes to the surface being of the same order of magnitude. This low O atom fractional surface coverage is due to the consumption of O atoms *via* their barrierless self-reaction, and also their reaction with O_2. Our model predicts that when the surface temperature is 20 K [O(ads)] and [C_2H_3CN(ads)] reach a relative steady-state fractional surface coverage of about 1:10 after dosage times of less than 1 s. We note that it is not possible to fit our experimental data with a pure ER model. If the ER1 and ER2 reaction probabilities are increased to fit the experimental data points between 40 and 60 K, the predicted yields between 14 and 30 K become far larger than the experimental data. Hence, as also concluded above, the LH mechanism must be contributing to the formation of C_3H_3NO.

Considering the form of Fig. 4, at a surface temperature of 100 K only acrylonitrile can adsorb on to the surface as shown by the desorption profile presented in Fig. 6. When gas-phase O atoms are incident upon this acrylonitrile ice, a reaction occurs generating C_3H_3NO *via* the ER1 mechanism. When experiments are carried out at surface temperatures below 70 K, O atoms can now adsorb on to the surface and the LH mechanism (Reaction 3) becomes active, increasing the yield of C_3H_3NO. For experiments at surface temperatures of 30 K and below, O_2 can also adsorb on to the surface. This opens up a competing pathway for O atom reactivity: O atoms can react with themselves, with O_2 (Reactions 2 and 6) to generate O_3, or with C_2H_3CN. The O + O_2 and O + O reactions are barrierless and compete very efficiently with the reaction between O and C_2H_3CN, thus the yield of C_3H_3NO is markedly reduced below 40 K.

5.1 Desorption energies

Adjusting the parameters of our model to fit the experimental data set (Fig. 4) allows us to extract desorption energies for each reactant. The desorption energy of O_2 critically affects the increase in yield of C_3H_3NO that is observed as the dosing temperature increases from 30 to 50 K; over this temperature range, O_2 desorbs from the surface and so Reactions (2) and (6) are inhibited. As a result, more O atoms are available to react with acrylonitrile to form C_3H_3NO. The lower bound we can place on the O_2 desorption energy represents the value required to predict this increase in C_3H_3NO yield. The upper bound of the O_2 desorption energy represents the desorption energy needed to predict the accompanying downturn in the yield of O_3 (Fig. 5).Of course, it is highly unlikely that the desorption energy of O_2 is single valued in the mixed-ice system under study. Noble et al. (2012) have shown that the desorption energy of O_2, on surfaces of astrochemical interest, is dependent upon the surface coverage. Our kinetic model predicts a steady-state O_2 surface coverage of 0.47 ML at 20 K after 1 s. The desorption energy of a 0.5 ML O_2 ice on an amorphous non-porous water substrate has been extracted to be 8.08 kJ mol^{-1} (972 K) (Noble et al. 2012) and so the value of 8.5 ± 0.8 kJ mol^{-1} (1020 ± 100 K) we extract here (Table 1) is in good agreement with the available literature data.

The desorption energy for O atoms extracted from our experimental data set is 14.2 ± 1.0 kJ mol^{-1} (1710 ± 120 K) and is in line with previous values extracted from experimental data by Kimber, Ennis & Price (2014), He & Vidali (2014), He et al. (2015a), and Minissale et al. (2016).

The desorption energy we extract for acrylonitrile from our model is 22.7 ± 1.2 kJ mol^{-1} (2730 ± 120 K). This value is similar to the desorption energies determined for propene, 21.4 ± 0.3 kJ mol^{-1} (2570 ± 40 K) and propyne, 20.8 ± 0.3 kJ mol^{-1} (2500 ± 40 K) (Ward & Price 2011; Kimber, Ennis & Price 2014) from multilayer mixed ices. As we observe, the desorption energy of acrylonitrile is expected to be slightly larger than propene and propyne due to the larger mass of the acrylonitrile molecule. However, our extracted desorption energy for acrylonitrile is significantly smaller than the previous estimation of 35 kJ mol^{-1} (4200 K) from a pure acrylonitrile ice (Toumi et al. 2016). The desorption energy extracted from our data set is essential for fitting the reduction in the yield of C_3H_3NO at dosing temperatures between 90 and 100 K (Fig. 4). If acrylonitrile does not start to desorb from the surface at 95 K, the ER1 mechanism will continue to generate C_3H_3NO at surface temperatures above 100 K, in clear contradiction to our experimental data. The desorption energy of a given molecule is directly related to the temperature at which the molecule desorbs from the surface. It has previously been determined that water desorbs from a pure ice between 160 and 180 K (Bolina, Wolff & Brown 2005). In the same study, the desorption energy of water was extracted to be 36.2 kJ mol^{-1} (4350 K). In our experiments acrylonitrile desorbs from the surface between 95 and 105 K (Fig. 6) and so its desorption energy must be significantly smaller than that of water. For these reasons, our value for the desorption energy of 22.7 ± 1.2 kJ mol^{-1} (2730 ± 120 K) for acrylonitrile seems perfectly appropriate under our experimental conditions. We believe part of the discrepancy between the desorption energy extracted for acrylonitrile here, and that extracted by Toumi et al. (2016), is due to the vastly different

heating rates used in the two sets of desorption experiments. In the earlier study, heating rates ranged from 0.5 to 3.5 K min^{-1}, almost two orders of magnitudes lower than the heating rate during our experiments. At our higher heating rates, and with a mixed ice on the surface, it is possible that the crystallization of acrylonitrile, observed at 94 and 135 K by Toumi et al. (2016), cannot take place and, upon reaching the crystallization temperature of 94 K, acrylonitrile desorbs from the surface. Thus, the desorption energy extracted in this paper represents the desorption energy of anamorphous acrylonitrile ice rather than the crystalline ice generated in the earlier experiments. In summary, adjusting the parameters of our model to fit the experimental data set allows the extraction of desorption energies of O_2, O, and acrylonitrile that are in agreement with related measurements in the literature.

5.2 Reaction probabilities and barriers

The reaction probabilities required to account for the yield of C_3H_3NO in our experiments are 0.007 ± 0.003 and 0.038 ± 0.004, for the LH and ER mechanisms, respectively (Table 1). In principle, these reaction probabilities provide information on the barrier to the reaction between O atoms and acrylonitrile on the surface. Simplistically, one could estimate the barrier of the reaction with which these probabilities are associated using an Arrhenius expression:

$$E_x/R = -T \ln(\rho_x) \quad (14)$$

where E_x/R is the reaction barrier in Kelvin and T is the surface temperature. However, as discussed below, care is required in extracting reaction barriers from such measured reaction probabilities. Specifically, for the ER pathway, we must first take account of the thermal energy of the gas-phase species and calculate an 'effective' temperature of the reactive event, recalling that the gas-phase species has a temperature T_g of 300 K. The effective temperature for the ER mechanism can be calculated (Minissale et al. 2013b) as:

$$T_{eff} = \mu \left(\frac{T_D}{m_s} + \frac{T_g}{m_g} \right) \quad (15)$$

Here μ is the reduced mass of the acrylonitrile/O atom system and m_s and m_g the masses of the molecule on the surface and in the gas phase, respectively. Our simulations show that the ER1 mechanism dominates the ER reactivity (Reaction 7) and the effective temperature for the ER1 mechanism, over our range of dosing temperatures, ranges from 222 to 245 K. This range of effective temperatures allow us to estimate an ER reaction barrier of 6.3 ± 0.6 kJ mol^{-1} (760 ± 70 K). Of course, in principle, we should include in our modelling the fact that the ER reaction probability will vary with the effective temperature. However, as discussed before, our experimental data do not provide sufficient constraints for such analysis (Minissale et al. 2013b). Hence, we assume ρ_{ER} is not a function of temperature and we should interpret ρ_{ER} as an average value over the temperature range studied. Reassuringly, since the effective temperature of the dominant ER1 pathway does not vary greatly over our range of surface temperatures (see above), this approximation is not unreasonable.

Consideration of the LH barrier is more complex. One could argue the reaction barrier for addition of O atoms to acrylonitrile on the surface should be independent of the pathway (LH or ER) by which the reactants encounter each other. However, in the LH pathway, the thermal energy available is lower than in the ER route, but, in compensation, the reactants are localized adjacent to each other and can have many encounters. More fundamentally, for the LH pathway, we must consider the possibility, at our low surface temperatures, that tunnelling of O atoms could be contributing to the passage from reactants to products. Indeed, we noted above that we cannot achieve a satisfactory fit to the experimental data if we enforce an Arrhenius temperature dependence for ρ_{LH}. Such an observation points at the possibility of O atom tunnelling being a significant reaction pathway in the reaction with acrylonitrile, as has been noted for other O atom reactions (Minissale et al. 2013a,b; Congiu et al. 2014; Minissale, Congiu & Dulieu 2014). Employing equation (14) with $\rho_{LH} = 0.007 \pm 0.003$ and a temperature range (over which the LH mechanism is operating) of 20–80 K gives a lower limit for the barrier height of 2.6 ± 1.4 kJ mol^{-1} (310 ± 170 K). This value is a lower limit as the barrier will be higher if tunnelling is indeed a significant route to the C_3H_3NO product. Reassuringly, the value of the barrier height we extract from the ER pathway is larger than the lower limit of the barrier height determined from the LH pathway.

In the gas phase, the reaction of acrylonitrile and O atoms proceeds over a barrier of 7.14 kJ mol^{-1} (859 K) (Upadhyaya et al. 1997) which is similar to the barrier we derive for the ER mechanism. This is not unexpected as the electronic structure of the physisorbed reactant will not be significantly perturbed from that of an isolated species and thus, the reactive ER encounter could be expected to proceed along a potential that is similar to that encountered in the gas phase.

In summary, consideration of the effective temperatures of the reactive encounters and the reaction probabilities allow us to extract a barrier for the ER reaction, which is comparable to the gas-phase value. A lower limit for the LH barrier can also be determined.

5.3 Mechanistic aspects

Acrylonitrile has two unsaturated centres, the C=C bond and the C≡N bond. If full saturation of acrylonitrile was achieved in our experiments, one would expect to observe a product at $m/z = 101$ resulting from the addition of three oxygen atoms. There is no evidence in our data for any reaction products involving the addition of more than one oxygen atom (see Supporting Information). If the site of the addition of this single oxygen atom was the cyanide group, we would also expect the addition of a second oxygen atom to occur at the C=C double bond, as such C=C bonds have been shown to be extremely reactive towards O atoms in previous experiments (Ward & Price 2011). Since only the addition of a single oxygen atom is observed, this strongly indicates the site of that addition is the C=C bond. To support this conclusion, we have performed additional experiments codepositing oxygen atoms with propionitrile (C_2H_5CN), a molecule structurally similar to acrylonitrile, except without the C=C bond. In these experiments, no addition of O atoms was observed, within the detection limits of our experiments. Similarly, no observable addition products were detected for the reaction of methylcyanide or cyanide ices with O atoms. Given the above data, it seems clear that the O atoms react with the C=C bond in acrylonitrile, not the CN moiety.

Previous work has shown that when ethene, the simplest molecule containing a C=C bond, is dosed on a graphite surface together with O atoms, a single oxygen addition is observed (Ward & Price 2011). These experiments identify the dominant product of this reaction as ethylene oxide, accompanied by a small amount of acetaldehyde (Fig. 7). If the reaction between O atoms and acrylonitrile forms analogous products to those formed with ethene, we would expect the C_3H_3NO to be primarily cyanoethylene oxide accompanied by a small amount of cyano-acetaldehyde or acetylcyanide (Fig. 7). In

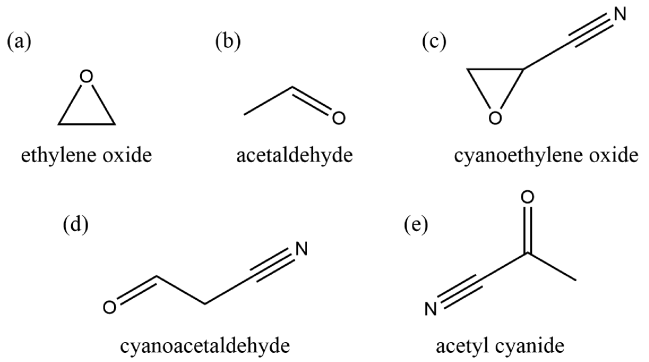

Figure 7. Chemical structures pertinent to the discussion of the reaction of O atoms with acrylonitrile.

support of this proposition, our experimental desorption data indeed hint that at least two isomers of the C_3H_3NO product are formed, as two desorption peaks are observed for this species (Fig. 3). The two desorption peaks indicate two different product-surface interaction energies, perhaps associated with different product structures. Our ideas regarding the precise form of the C_3H_3NO product are also in line with the gas-phase pathway for the reaction of O atoms and acrylonitrile, discussed above, where the major product is thought to form *via* a biradical species, which subsequently forms an epoxidering (Fig. 1, Upadhyaya et al.1997).

In conclusion, structural considerations and the reactivity of related species, indicate the site of O atom addition to acrylonitrile is the C=C bond, favouring a nascent product containing an epoxidering. This reactive species then probably rearranges to a more stable linear structure.

6 ASTROPHYSICAL IMPLICATIONS

The results presented in this paper show that oxygen atoms can readily add to acrylonitrile on cold interstellar dust grain analogues under conditions mimicking the ISM. The fluence of oxygen atoms used in this experiment has been previously determined to be equivalent to 10^5–10^6 yr of exposure to O atoms in an interstellar cloud (Ward & Price 2011). It is therefore possible that this pathway is active on the surface of dust grains in the ISM. This pathway is not only relevant to dense interstellar clouds, where grain temperatures are 10–20 K, but also to the warm-up phase of these clouds, since acrylonitrile will remain on the grains until the temperature reaches approximately 100 K. We hypothesize that during the warm-up phase of a cloud, when dust temperatures approach 140 K, cyanoethyleneoxide, and perhaps acetylcyanide, could be observed in the gas phase. A confirmed detection of one of these molecules would provide further support for the reaction of acrylonitrile and O atoms being an active pathway on interstellar dust grains. Indeed, since the coverage of molecular oxygen will be markedly lower in the interstellar situation than in our experiments, one would expect the net yield of products, per oxygen atom for a given coverage of acrylonitrile, to be higher.

Our results confirm that the LH mechanism is active under experimental conditions relevant to surface chemistry in the ISM; it is the LH mechanism which is of particular relevance in this situation as relative coverages of the reactant species are low. Of course, acrylonitrile will have lower surface concentrations in the ices present on interstellar dust grains than molecules, such as methane, CO, and ammonia. However, more generally, our results show that reactions with O atoms are likely to be efficient on interstellar dust grains for a wide range of molecules containing carbon–carbon multiple bonds. Conversely, reactions of O atoms with the CN group are likely to be less efficient. Indeed, we note that the reaction probability between acrylonitrile and O atoms is larger than that of the reaction between O atoms and CO (Minissale et al. 2013b).

Prior to the recent experimental focus on the surface chemistry of oxygen atoms, it was implicit that dominant atomic chemistry involved in the route to molecular complexity on interstellar ices involved H atoms. However, recent surface science experiments show that oxygen atoms have a significantly larger desorption energy than had been previously predicted by theory. This large desorption energy allows oxygen atoms to develop appreciable surface concentrations at surface temperatures up to 70 K. Therefore, the chemistry of O atoms can continue on grain surfaces during the first part of the warm-up phase of the dust in interstellar clouds, after all hydrogen atoms have desorbed from the grains (Herbst 2014). Indeed, previous authors have pointed out that under certain interstellar conditions, oxygen atoms can become the major surface species in atomic form (Congiu et al. 2014).

7 CONCLUSIONS

The results presented in this paper report the first laboratory study of the heterogeneous reactions of acrylonitrile and oxygen atoms at low surface temperatures relevant to the ISM. Our data show that a single oxygen atom can add efficiently to acrylonitrile on surfaces at temperatures below 100 K. In considering the yield of the reaction of O atoms with acrylonitrile, it is important to consider the competing reaction of O atoms with O_2. At surface temperatures of 14 and 20 K, particularly relevant to the surface chemistry of cold interstellar dust grains, there is still an appreciable product flux involving oxygen atom addition to acrylonitrile. We hypothesize that the major isomer of the initial addition product is cyanoethylene oxide.

ACKNOWLEDGEMENTS

We would like to thank University College London and the Max-Planck Institute for Astronomy for support of HJK. SDP and HJK also acknowledge support from the European Commission's Seventh Framework Programme (FP7/2007–2013) under the LASSIE training network (Project ID: 238258). The authors also acknowledge many helpful discussions with Francois Dulieu, Emmanuel Congiu, Marco Minissale, and others at Université de Cergy-Pontoise.

REFERENCES

Bell M.B., Feldman P.A., Travers M.J., McCarthy M.C., Gottlieb C.A., Thaddeus P., 1997, ApJ, 483, L61
Bell M.B., Watson J.K.G., Feldman P.A., Travers M.J., 1998, ApJ, 508, 286
Bergeron H., Rougeau N., Sidis V., Sizun M., Teillet-Billy D., Aguillon F.,2008, J. Phys. Chem. A, 112, 11921
Bergin E.A., Tafalla M., 2007, ARA&A, 45, 339
Bolina A.S., Wolff A.J., Brown W.A., 2005, J. Phys. Chem. B, 109, 16836
Cartledge S.I.B., Lauroesch J.T., Meyer D.M., Sofia U.J., 2004, ApJ, 613, 1037
Congiu E. et al., 2014, Faraday Discuss., 168, 151
Gardner F.F., Winnewisser G., 1975, ApJ, 195, L127
Garrod R.T., Weaver S.L.W., Herbst E., 2008, ApJ, 682, 283
Gerry M.C.L., Yamada K., Winnewisser G., 1979, J. Phys. Chem. Ref. Data, 8, 107
Hasegawa T.I., Herbst E., Leung C.M., 1992, ApJS, 82, 167

He J., Vidali G., 2014, Faraday Discuss., 168, 517
He J., Shi J., Hopkins T., Vidali G., Kaufman M.J., 2015a, ApJ, 801, 120
He J., Vidali G., Lemaire J.L., Garrod R.T., 2015b, ApJ, 799, 9
Herbst E., 2014, Faraday Discuss., 168, 617
Hincelin U., Wakelam V., Hersant F., Guilloteau S., Loison J.C., Honvault P., Troe J., 2011, A&A, 530, A61
Hudson R.L., Moore M.H., 2004, Icarus, 172, 466
Jenkins E.B., 2009, ApJ, 700, 1299
Johansson L.E.B.et al., 1984, A&A, 130, 227
Kimber H.J., Ennis C.P., Price S.D., 2014, Faraday Discuss, 168, 167
Kimber H.J., 2016, PhD theses, University College London, London
Matthews H.E., Sears T.J., 1983, ApJ, 272, 149
Minissale M. et al., 2013a, Phys. Rev. Lett., 111, 053201
Minissale M., Congiu E., Manico G., Pirronello V., Dulieu F., 2013b, A&A, 559, A49
Minissale M., Congiu E., Dulieu F., 2014, J. Chem. Phys., 140, 074705
Minissale M., Congiu E., Dulieu F., 2016, A&A, 585, A146
Newson K.A., Luc S.M., Price S.D., Mason N.J., 1995, Int. J. Mass Spectr. Ion Process., 148, 203
Noble J.A., Congiu E., Dulieu F., Fraser H.J., 2012, MNRAS,421,768
Stantcheva T., Shematovich V.I., Herbst E., 2002, A&A, 391, 1069
Stein S.E., 2015, NIST mass spec data center, in:Linstrom P.J., Mallard W.G., eds, NIST Chemistry WebBook, NIST Standard Reference Database Number 69, National Institute of Standards and Technology, Gaithersburg MD. Available at: http://webbook.nist.gov (retrieved 2015 December 4)
Straub H.C., Renault P., Lindsay B.G., Smith K.A., Stebbings R.F., 1996, Phys. Rev. A, 54, 2146
Theule P., Borget F., Mispelaer F., Danger G., Duvernay F., Guillemin J.C., Chiavassa T., 2011, A&A, 534, A64
Toumi A., Piétri N., Chiavassa T., Couturier-Tamburelli I., 2016, Icarus, 270, 435
Upadhyaya H.P., Naik P.D., Pavanaja U.B., Kumar A., Vatsa R.K., Sapre A.V., Mittal J.P., 1997, Chem. Phys. Lett., 274, 383
Vuitton V., Yelle R.V., McEwan M.J., 2007, Icarus, 191, 722
Ward M.D., Price S.D., 2011, ApJ, 741, 121
Ward M.D., Hogg I.A., Price S.D., 2012, MNRAS, 425, 1264
Whittet D.C.B., 2010, ApJ, 710, 1009
Willacy K., Allen M., Yung Y., 2016, ApJ, 829, 79
Williams D.A., Cecchi-Pestellini C., 2016, Dust-related chemistry in space, in Chemistry of Cosmic Dust. Royal Society of Chemistry, Cambridge, p. 1

SUPPORTING INFORMATION

Supplementary data are available at *MNRAS* online.

Please note: Oxford University Press is not responsible for thecontent or functionality of any supporting materials supplied bythe authors. Any queries (other than missing material) should bedirected to the corresponding author for the article.

This paper has been typeset from a Microsoft Word file prepared by the author.